Structural Engineering and Mechanics, *Vol. 48, No. 1 (2013) 103-124*
DOI: http://dx.doi.org/10.12989/sem.2013.48.1.103

Hygrothermal effects on dynamic instability of a laminated plate under an arbitrary pulsating load

Hai Wang[1], Chun-Sheng Chen[2] and Chin-Ping Fung[*3]

[1]*Mechanical Engineering, Ming Chi University of Technology,Tai-Shan 24301, Taiwan*
[2]*Mechanical Engineering, Lunghwa University of Science and Technology, Gui-Shan 33306, Taiwan*
[3]*Mechanical Engineering, Oriental Institute of Technology, Pan-Chiao 22061, Taiwan*

(Received July 11, 2012, Revised September 17, 2013, Accepted October 2, 2013)

Abstract. This paper studies the static and dynamic characteristics of composite plates subjected to an arbitrary periodic load in hygrothermal environments. The material properties of composite plates are depended on the temperature and moisture. The governing equations of motion of Mathieu-type are established by using the Galerkin method with reduced eigenfunction transforms. A periodic load is taken to be a combination of axial pulsating load and bending stress in the example problem. The regions of dynamic instability of laminated composite plates are determined by solving the eigenvalue problems based on Bolotin's method. The effects of temperature rise and moisture concentration on the dynamic instability of laminated composite plates are investigated and discussed. The influences of various parameters on the instability region and dynamic instability index are also investigated. The numerical results reveal that the influences of hygrothermal effect on the dynamic instability of laminated plates are significant.

Keywords: dynamic instability; hygrothermal effect; laminated plates ; Galerkin method; bolotin's method

1. Introduction

Most laminated composite plates can offer a higher ratio of strength and stiffness to weight than traditional metal plates do and thus have been widely used in many engineering industries. When a plate is subjected to periodic loads, it may experience the dynamic instability due to parametric resonance. It is important in theory and practice to accurately determine the region of dynamic stability of the plate, and a careful investigation of this phenomenon is necessary. Numerous references pertaining to the parametric resonance of plates can be found in the books written by Bolotin (1964) and Evan-Ivanowski (1976). The dynamic stability of laminate composite plates has been studied by many researchers using various approximate methods (Chen *et al*. 2009, Chakrabarti 2008, Dey and Sinqha 2006, Patel *et al*. 2009). In addition, the stability of composite laminate plates in hygrothermal environments has been also studied by many researchers. During the service life, the elevated temperature and moisture will reduce the elastic modulus and degrade the strength of the composite laminated material (Gigliottia *et al*. 2006,

∗Corresponding author, Professor, E-mail: cpfung@mail.oit.edu.tw

http://www.techno-press.org/?journal=sem&subpage=8 ISSN: 1225-4568 (Print), 1598-6217 (Online)

Kumar and Singh 2012, Rao and Sinha 2004a). In such hygrothermal circumstances, the stresses will be induced in the laminated composite plates and consequently lead to the change in mechanical behaviors. So the quantity of the research in stability behavior of laminated composite plates in hygrothermal environments considerably increased in recent years.

Parhi *et al*. (2001) presented the dynamic behavior of delaminated composite shells subjected to a hygrothermal environment. The analysis took into account the lamina material properties at elevated moisture concentration and temperature. Newmark's direct integration scheme was used to solve the dynamic equation of equilibrium at every time step during the transient analysis. The results showed a reduction in the fundamental frequency with an increase in the percentage of uniform moisture content as well as temperature for any size of delamination considered. The effect of hygrothermal conditions on the nonlinear vibration (Huang *et al*. 2004) and dynamic response (Shen *et al*. 2004) of laminate plates resting on an elastic foundation were studied. The material properties of the composite were affected by the variation of temperature and moisture based on a micromechanical model of a laminate. The equations of motion were solved by an improved perturbation technique to determine nonlinear frequencies and dynamic responses of laminated plates. The results showed that the hygrothermal environment has a significant effect on the natural frequency, nonlinear to linear frequency ratios and dynamic responses of the plate.

Rao and Sinha (2004b) presented the effects of temperature and moisture on the free vibration and transient response of composites. The analysis accounted for the degradation of composite properties due to both temperature and moisture concentration. The numerical results for the natural frequencies and transient response of multidirectional composites under the effect of both temperature and moisture concentration were presented and discussed. The active stiffening and active compensation analyses were carried out to present the influence of active stiffness on the dynamic behavior of piezo-hygro-thermo-elastic laminates by Raja *et al*. (2004). Through a parametric study, the influence of active stiffening and active compensation effects on the dynamics of laminated plates and shells were highlighted. The reduction in natural frequencies of laminates due to hygrothermal strain is actively compensated by active stiffening. Dynamic responses of an orthotropic plate subjected to hygrothermal environments were optimized by Cho (2009). The dynamic deflection and natural frequency were minimized by optimizing design variables. The dynamic analysis of orthotropic plate under temperature and humidity boundary conditions was presented. The nonlinear dynamic response of laminated shells with imperfection in hygrothermal environments was studied by Nanda and Pradyumna (2011). The theoretical formulations were based on the first-order shear deformation theory and von Karman nonlinear kinematics. An imperfection function capable of modeling a variety of sine type, global type, and localized type imperfections was used. The effects of moisture and temperature on the nonlinear free vibration and transient responses of laminated composite shells were studied. There is no literature investigating the dynamic behavior of shear deformable laminated plates subjected to an arbitrary periodic load under hygrothermal environmental conditions.

The dynamic vibration behavior of composite plates under arbitrary initially stresses was analyzed by the author *et al*. (2009). Then the dynamic instability of laminated plates under arbitrary in-plane periodic loads in thermal environments (Chen *et al*. 2013) was presented. The governing partial differential equations of motion were established by a perturbation technique. The effects of temperature, modulus ratio and dynamic load on the dynamic instability of laminated plates were investigated. In the present study, the governing equations of laminated plate in arbitrary periodic loads under hygrothermal environmental conditions were further derived. The Galerkin method was applied to the governing partial differential equations to yield

ordinary differential equations. The dynamic load was taken to be a combination of a periodic bending stress and a periodic axial stress in the example problems. The material properties of laminated plate were assumed to be functions of temperature and moisture, and both ambient temperature and moisture were assumed to feature a uniform distribution. Based on Bolotin's method, a set of ordinary differential equations with periodic coefficients of Mathieu-Hill type was formulated to obtain the boundaries of the regions of dynamic instability of laminated composite plates. An eigenvalue problem was solved to determine the boundary frequencies for the boundaries of instability regions. And the effects of temperature rise, moisture concentration and fiber volume fraction on the region of hygrothermal dynamic stability were studied.

2. Theoretical formulations

The dynamic equations of a composite plate with uniform thickness h in a general state of general time-varying initial stress are established in this study. Hamilton's principle as described by Brunell and Robertson (1974), Chen *et al*. (2006) is applied to derive the governing equations of motion of the plate

$$\delta\int_{t_0}^{t_1}(U_s - K_t - W_i - W_e)dt = 0 \tag{1}$$

where U_t is the strain energy, $U_t = \int_{V_0} \sigma_{ij}\varepsilon_{ij}dV$

K_t is the kinetic energy, $K_t = \frac{1}{2}\int_{V_0}\rho\dot{v}_i\dot{v}_i dV$

W_e is the work of external forces, $W_e = \int_{S_0} p_i v_i dS$

W_i is the work of internal forces, $W_i = \int_{v_o} X_i v_i dV$

The application of the variational principle leads to the general equations and boundary conditions. σ_{ij} is the stress referred to the material coordinates; ε_{ij} is the strain referred to the material coordinates; v_i is the displacement referred to the spatial frame; X_i is the body force per unit initial volume and p_i is the external force per unit initial surface area. Then taking the variation, integrating the kinetic energy term by parts with respected to time, Eq. (1) becomes

$$\int_{t_0}^{t_1}[\int_{V_0}(\sigma_{ij}\delta\varepsilon_{ij} - X_i\delta v_i - \rho\ddot{v}\delta v_i)dV - \int_{S_0}(p_i\delta v_i)dS]dt = 0 \tag{2}$$

In order to account for the transverse shear deformation and rotary inertia effects in the laminated composite plate, the incremental displacements are assumed to be of the following forms based on the first-order shear deformation plate theory

$$\begin{aligned} v_x(x, y, z, t) &= u_x(x, y, t) + z\varphi_x(x, y, t) \\ v_y(x, y, z, t) &= u_y(x, y, t) + z\varphi_y(x, y, t) \\ v_z(x, y, z, t) &= w_z(x, y, t) \end{aligned} \tag{3}$$

where u_x, u_y and w_z are displacements at the midplane in the x, y and z directions, respectively; φ_x

and φ_y are rotation angles about y and x axes, respectively. The x and y axes of the coordinate system are set to coincide with the two edges of the laminate.

The constitutive matrix equation for a typical k^{th} layer with reference to the material-axis coordinate system can be written as

$$\begin{bmatrix}\sigma_{xx}\\ \sigma_{yy}\\ \sigma_{xy}\\ \sigma_{yx}\\ \sigma_{zx}\end{bmatrix}=\begin{bmatrix}C_{11}&C_{12}&C_{16}&0&0\\ C_{12}&C_{22}&C_{26}&0&0\\ C_{16}&C_{26}&C_{66}&0&0\\ 0&0&0&C_{44}&C_{45}\\ 0&0&0&C_{45}&C_{55}\end{bmatrix}\begin{bmatrix}\varepsilon_{xx}-\alpha_{xx}\Delta T-\beta_{xx}\Delta C\\ \varepsilon_{yy}-\alpha_{yy}\Delta T-\beta_{yy}\Delta C\\ \varepsilon_{xy}-\alpha_{xy}\Delta T-\beta_{xy}\Delta C\\ \varepsilon_{yx}\\ \varepsilon_{zx}\end{bmatrix} \tag{4}$$

where C_{ij} is the material stiffness of lamina. ΔT and ΔC are respectively the rise in temperature and moisture concentration; α_{xx}, α_{yy} and α_{xy} are transformed thermal expansion coefficients in the principal material directions; hygro coefficients β_{xx}, β_{yy} and β_{xy} are moisture expansion coefficients. If V_f and V_m are the fiber and matrix volume fractions of a plate, the two volume fractions are related by

$$V_f + V_m = 1 \tag{5}$$

Then, ρ_f and ρ_m are fiber and matrix mass density, and the mass density of a laminate is obtained by

$$\rho = V_f \rho_f + V_m \rho_m \tag{6}$$

The material properties of laminate are function of temperature and moisture. In terms of a micro-mechanical model of the laminate, the thermal expansion coefficients in the longitudinal and transverse directions can be written as (Tsai and Hahn 1980)

$$\alpha_{xx} = \frac{V_f E_f \alpha_f + V_m E_m \alpha_m}{V_f E_f + V_m E_m}$$

$$\alpha_{yy} = (1+\upsilon_f) V_f \alpha_f + (1+\upsilon_m) V_m \alpha_m - \upsilon_{xy} \alpha_{xx} \tag{7}$$

where E_f, α_f and υ_f are Young modulus, thermal expansion coefficient and Poisson ratio of the fiber, respectively. E_m, α_m and υ_m are corresponding properties for the matrix. The Poisson ratio υ_{xu} is

$$\upsilon_{xy} = V_f \upsilon_f + V_m \upsilon_m \tag{8}$$

The longitudinal and transverse coefficients of humid expansion of a lamina may be written as

$$\beta_{xx} = \frac{V_f E_f c_{fm} \beta_f + V_m E_m \beta_m}{E_{xx}(V_f \rho_f c_{fm} + V_m \rho_m)} \rho$$

$$\beta_{yy} = \frac{V_f (1+\upsilon_f) c_{fm} \beta_f + V_m (1+\upsilon_m) \beta_m}{V_f \rho_f c_{fm} + V_m \rho_m} \rho - \upsilon_{xy} \beta_{xx} \tag{9}$$

where c_{fm}, β_f and β_m is the moisture concentration ratio, fiber and matrix humid expansion coefficient, respectively. Thus, the material properties of lamina can be expressed as

$$E_{xx} = V_f E_F + V_m E_m$$

$$\frac{1}{E_{yy}} = \frac{V_f}{E_f} + \frac{V_m}{E_m} - V_f V_m \frac{\upsilon_f^2 E_m / E_f + \upsilon_m^2 E_f / E_m - 2\upsilon_f \upsilon_m}{V_f E_f + V_m E_m}$$

$$\frac{1}{G_{xy}} = \frac{V_f}{G_f} + \frac{V_m}{G_m} \tag{10}$$

The general time-dependent initial stress system applied to the rectangular laminated plate is assumed to have the form:

$$\sigma_{ij} = \sigma_{\mathrm{ij}}^{\mathrm{n}} + 2z\sigma_{\mathrm{ij}}^{\mathrm{m}} / h$$

$$= (\sigma_{ij}^S + \sigma_{ij}^D \cos\varpi t) + 2z(\sigma_{ij}^{Sm} + \sigma_{ij}^{Dm} \cos\varpi t)/h \quad (i, j = x, y, z) \tag{11}$$

which is consisted of the spatially uniform longitudinal, transverse, shear, bending and twisting stress. Here σ_{ij}^S and σ_{ij}^D are the static and dynamic components of the periodic normal or shear stress $\sigma_{\mathrm{ij}}^{\mathrm{n}}$; σ_{ij}^{Sm} and σ_{ij}^{Dm} are the static and dynamic components of the periodic pure bending or torsion stress $\sigma_{\mathrm{ij}}^{\mathrm{m}}$; ϖ is the disturbing frequency of the dynamic loads. Substitute Eqs. (3)-(11) into Eq. (2), perform all necessary partial integrations and group terms together by the displacements variation, the dynamic equations of rectangular laminated plates are obtained as follows

$$(L_1 + P_1 + T_1 + H_1)_{,\mathrm{x}} + (L_2 + P_2 + T_2 + H_2)_{,y} + f_x = I_1 \ddot{u}_x \tag{12}$$

$$(L_2 + P_3 + T_3 + H_3)_{,x} + (L_3 + P_4 + T_4 + H_4)_{,y} + f_y = I_1 \ddot{u}_y \tag{13}$$

$$(L_4 + P_5 + T_5 + H_5)_{,x} + (L_5 + P_6 + T_6 + H_6)_{,y} + f_z = I_1 \ddot{w} \tag{14}$$

$$(L_6 + P_7 + T_7 + H_7)_{,x} + (L_7 + P_8 + T_8 + H_8)_{,y} - L_8 - P_9 + m_x = I_1 \ddot{\varphi}_{\mathrm{x}} \tag{15}$$

$$(L_7 + P_{10} + T_9 + H_9)_{,x} + (L_9 + P_{11} + T_{10} + H_{10})_{,y} - L_{10} - P_{12} + m_y = I_1 \ddot{\varphi}_{\mathrm{y}} \tag{16}$$

The coefficients of above equations are given in the Appendix.

3. Hygrothermal dynamic instability analysis

As the dynamic behavior of a laminated plate in hygrothermal environments is affected by many parameters, it is difficult to study all various cases. Hence, this study investigates the dynamics behavior of a simply supported rectangular laminated plate subjected to a periodic spatially uniform in-plane stress which consists of a pulsating longitudinal normal stress and a pure bending stress. With assuming all other stresses zero, the stress system Eq. (11) is reduced to

$$\sigma_{xx} = \sigma_{xx}^n + 2z\sigma_{xx}^m/\mathrm{h} = \sigma_{\mathrm{n}} + 2z\sigma_m / h \tag{17}$$

Here $\sigma_n = \sigma_{xx}^S + \sigma_{xx}^D \cos\varpi t = \sigma^S + \sigma^D \cos\varpi t$ and $\sigma_m = \sigma_{xx}^{Sm} + \sigma_{xx}^{Dm} \cos\varpi t = \sigma^{Sm} + \sigma^{Dm} \cos\varpi t$. The

static and dynamic stress components, σ^S, σ^D, σ^{Sm} and σ^{Dm}, are taken to be constants. The nonzero loads are only $N_{xx} = h\sigma_n$, $M_{xx} = Sh^2\sigma_m/6$, $M^*_{xx} = h^3\sigma_n/12$, where bending ratio $S = \sigma_m / \sigma_n$ is the ratio of bending stress to normal stress. The hygrothermal coupling in governing equations vanishes.

The boundaries of the rectangular plate are simple supported along x=0 and a, y=0 and b. To satisfy the simply supported boundary conditions, the following shape modes of displacement fields are used.

$$u_x = \sum\sum h U_{mn}(t) \cos(m\pi x/a) \sin(n\pi y/b)$$
$$u_y = \sum\sum h V_{mn}(t) \sin(m\pi x/a) \cos(n\pi y/b)$$
$$w_z = \sum\sum h W_{mn}(t) \sin(m\pi x/a) \sin(n\pi y/b)$$
$$\varphi_x = \sum\sum \Psi_{xmn}(t) \cos(m\pi x/a) \sin(n\pi y/b)$$
$$\varphi_y = \sum\sum \Psi_{ymn}(t) \sin(m\pi x/a) \cos(n\pi y/b) \quad (18)$$

Assume that the $\Delta(t)=[U_{mn},V_{mn},W_{mn},\Psi_{xmn},\Psi_{ymn}]^T = \bar{\Delta} f(t)$, in which the Δ and $\bar{\Delta}$ denote the time dependent and independent displacement vector, respectively. Substituting the assumed displacement field Eq. (18) into the Eqs. (12)-(16) and applying Galerkin method lead to the following matrix equation of motion

$$\{([K]-[T]-[H]+[G])\, f(t)+[M]\,(d^2 f(t)/dt)\}\,\bar{\Delta}=0 \quad (19)$$

in which [K], [T], [H], [G] and [M] are the respective elastic stiffness matrix, thermal effect matrix, humid effect matrix, geometric stiffness matrix and mass matrix. The system Eq. (19) is related to the eigenvalue problems of the buckling, vibration and dynamic instability.

To analyze the buckling of laminated plates in hygrothermal environments, the inertia term [M] and $f(t)$ in Eq. (19) are set to be zero and one, respectively. The eigenvalue equation for determining the buckling load is obtained as follows.

$$\{[K]-[T]-[H]+[G])\}\{\bar{\Delta}\}=\{0\} \quad (20)$$

The condition for the existence of a non-trivial solution is that the determinant of the coefficients is zero. The critical buckling load can be determined from the solution

$$\left|([K]-[T]-[H])-P_{cr}[G]\right|=0 \quad (21)$$

where P_{cr} is the static critical buckling load of the plate subjected to a uniaxial in-plane load. The governing equations of the free vibration of laminated plates in hygrothermal environments are obtained from Eq. (19) by setting $f(t)= e^{i\omega t}$

$$\{([K]-[T]-[H]+[G])-\omega^2[M]\}\,\bar{\Delta}=0 \quad (22)$$

The roots of the determinant of the coefficients of Eq. (22) are the natural frequencies of the laminated plate. The dynamic stability analysis of the laminated plate under a non-zero periodic stress in Eq. (17) is given next. The nonzero stress resultant N_{xx} can be obtained by integrating Eq. (17) with respect to variable z.

$$N_{xx}=-(\alpha_S P_{cr}+\alpha_D P_{cr}\cos\varpi t) \tag{23}$$

where $\alpha_S=h\sigma_{xx}^{S}/P_{cr}$ and $\alpha_D=h\sigma_{xx}^{D}/P_{cr}$ are static and dynamic load parameters, respectively. Let $[C]=[K]-[T]-[H]$. Substituting Eq. (23) into Eq. (19) gives

$$\{[C]+\alpha_S P_{cr}[G]^*+\alpha_D P_{cr}[G]^*\cos\varpi t)f(t)+[M](d^2 f(t)/dt)\}\bar{\Delta}=0 \tag{24}$$

which represents a second-order ordinary differential equation with periodic coefficients of Mathieu-Hill type. To determine the regions of dynamic instability, Bolotin's method (1964) is used. As the boundaries of primary instability region are usually more important in practicality than those of secondary instability region, and the solutions of the first-order approximation (a_1 and b_1) of the primary instability region of the dynamic stability is sufficiently accuracy (Chen and Yang 1990), only the first-order solution of primary instability region is considered in this study and is given by

$$[C]+\alpha_S P_{cr}[G]^* \pm \tfrac{1}{2}\alpha_D P_{cr}[G]^* - \tfrac{1}{4}\varpi^2[M]=0 \tag{25}$$

4. Results and discussion

In this study, the hygrothermal effect on dynamic vibration of a laminated plate is investigated. To validate the accuracy of present computer program, the minimum vibration frequency, critical buckling load in a thermal environment, and excitation frequencies of primary instability region are presented in Tables 1-4 and compared with solutions from other investigators. The data show that the the present results agree well with those obtained by Liu and Huang (1996), Patel *et al*. (2002), Wang and Dawe (2002).

In the following tables and figures, the influence of various parameters, including temperature, moisture, fiber volume fraction and bending stress, on the dynamic instability response of an eight-layers cross-ply laminated plate in hygrothermal environmental conditions is discussed. The

Table 1 Comparison of vibration frequencies of a four-layered cross-ply laminated plate in thermal environment

T_o	Source	α_{xx}/α_{yy}			
		-0.05	0.1	0.2	0.3
-50	Liu's results	15.149	15.247	15.320	15.394
	Present results	15.165	15.277	15.351	15.425
0	Liu's results	15.150	15.150	15.150	15.150
	Present results	15.179	15.179	15.179	15.179
50	Liu's results	15.164	15.052	14.978	14.902
	Present results	15.193	15.081	15.006	14.930

Table 2 Comparison of critical load ratio of a cross-ply laminated plate in thermal environment

Source	Temperature (^oC)				
	300	325	350	375	400
Patel's results	1	0.9954	0.9313	0.8650	0.8300
Present results	1	0.9933	0.9422	0.8885	0.8567

Table 3 Comparison of critical load ratio of a laminated plate in moisture environment

Source	Moisture concentration (%)						
	0	0.25	0.5	0.75	1	1.25	1.5
Patel's results	1	0.9863	0.9731	0.9606	0.9487	0.9380	0.9273
Present results	1	0.9863	0.9732	0.9607	0.9489	0.9383	0.9277

Table 4 Excitation frequencies for a symmetrically four-layer cross-ply laminate plate with various static and dynamic loads

α_S	α_D	Wang's results		Present results	
		ω^U	ω^L	ω^U	ω^L
0.0	0.0	144.57	144.57	144.36	144.36
0.0	0.3	155.03	133.29	155.64	133.79
0.0	0.6	164.83	120.95	165.12	121.45
0.0	0.9	174.08	107.21	174.43	107.63
0.0	1.2	182.87	91.43	183.21	91.86
0.0	1.5	191.25	72.28	191.75	72.62
0.2	0.06	131.71	126.86	132.12	127.26
0.4	0.12	117.45	106.24	117.96	106.82
0.6	0.18	101.20	80.49	101.84	81.10
0.8	0.24	81.78	40.89	82.31	41.32

temperature-dependent graphite/epoxy composite material properties are (Adams and Miller 1977; Bowles and Tompkins 1989, Shen 2001)

E_f =230 GPa, G_f =9 GPa, $\alpha_f = -0.54\times10^{-6}/^oC$, υ_f =0.203, ρ_f =1750 kg/m^3, β_f =0, c_{fm} =0, α_m = $45\times10^{-6}/^oC$, υ_m =0.34, ρ_m =1200 kg/m^3, $\beta_m = 2.68\times10^{-3}/wt\%H_2O$, E_m = $(3.51-0.003\times(25+\Delta T)-0.142\times\Delta C)$ GPa

The hygrothermal dynamic stability behaviors of laminate plates are investigated based on the procedure described in the previous section. The nondimensional vibration frequency ($\Omega = 10\omega b^2\sqrt{\rho_f/h^2E_f}$) and buckling coefficient ($K=100b^2N_{xx}/E_f$) are defined and used throughout the study. The non-dimensional coefficients of excitation frequency Ω, the instability region $\Delta\Omega=\Omega^U-\Omega^L$ and the dynamic instability index $\Omega_{DI}=\Delta\Omega/(\omega_{nf}K_{cr})$ are defined for the study of dynamic instability. Here Ω^U and Ω^L are the upper and lower boundary excitation frequency, respectively; ω_{nf} and K_{cr} are the dimensionless fundamental vibration frequency and critical buckling load. The dynamic instability index Ω_{DI}, an instability measure of the laminate plates under hygrothermal environments, represents a relationship between the instability region, fundamental vibration frequency, and static critical buckling load. The influence of various parameters of the laminated plate on its hygrothermal dynamic instability behaviors is examined and discussed next.

The effect of temperature, moisture, and fiber volume fraction on the buckling load and vibration frequency of laminated plates are presented in Tables 5-6. The buckling load and vibration frequency of laminated plates decrease as moisture and temperature increase and fiber volume fraction decreases. When the moisture or temperature increases, the buckling load and vibration frequency of laminated plates without fiber reinforced decrease significantly. The effects

of static load parameters on the excitation frequency ratio Ω/ω_{nf} are presented in Fig. 1, in which $\alpha_D/|\alpha_s|=0.3$. The excitation frequency ratio is independent of fiber volume fraction and hygrothermal condition. When the compressive static load ($\alpha_s>0$) increases, the upper and lower boundary of Ω/ω_{nf} decrease and the tensile static load ($\alpha_s<0$) has a reverse effect. Meanwhile, the distance between the two boundaries increases with the static load parameter. The figure also shows that the primary instability onset for $\alpha_s=0$ occurs at Ω equal to $2\omega_{nf}$, i.e., $\Omega/\omega_{nf}=2$, where $\alpha_D=0$. The onset of instability and instability width with static load factor can be further seen in Fig. 2, where the values of static load parameter α_s are set to be -0.4, 0 and 0.4. The figure shows that the instability onset occurs at Ω equal to 2.3664, 2.0 and 1.5492, respectively. It is evident that the compressive static load ($\alpha_s>0$) produces a softening effect on the excitation frequency ratio and

Table 5 Effect of temperature on buckling load and vibration frequency of a eight-layered cross-ply laminated plate (a/b=1, a/h=10, S=0, ΔC =0)

	V_f	Temperature rise(^oC)			
		0	50	100	150
K_{cr}	0	5.0687	4.8377	4.6075	4.3782
	0.1	11.6571	11.3883	11.1178	10.8453
	0.2	17.4845	17.1472	16.8038	16.4534
	0.3	23.0311	22.6150	22.1880	21.7487
	0.4	28.6316	28.1347	27.6222	27.0925
	0.5	34.5830	34.0079	33.4128	32.7955
ω_{nf}	0	8.5414	8.3444	8.1435	7.9382
	0.1	12.6661	12.5192	12.3696	12.2171
	0.2	15.1831	15.0359	14.8846	14.7286
	0.3	17.0710	16.9161	16.7556	16.5890
	0.4	18.6615	18.4989	18.3297	18.1530
	0.5	20.1235	19.9555	19.7801	19.5966

Table 6 Effect of moisture concentration on buckling load and vibration frequency of a eight-layered cross-ply laminated plate (a/b=1, a/h=10, S=0, ΔT =0)

	V_f	Moisture concentration (%)			
		0	1	2	3
K_{cr}	0	5.0687	3.6978	2.4270	1.2564
	0.1	11.6571	10.1178	8.6877	7.3665
	0.2	17.4845	15.7196	14.0734	12.5453
	0.3	23.0311	20.9919	19.0840	17.3065
	0.4	28.6316	26.2585	24.0343	21.9577
	0.5	34.5830	31.7873	29.1655	26.7160
ω_{nf}	0	8.5414	7.2954	5.9103	4.2524
	0.1	12.6661	11.8002	10.9345	10.0688
	0.2	15.1831	14.3964	13.6217	12.8610
	0.3	17.0710	16.2978	15.5395	14.7982
	0.4	18.6615	17.8714	17.0978	16.3425
	0.5	20.1235	19.2930	18.4802	17.6872

reduces the onset of instability region, on the other hand, the tensile static load (α_s <0) has a reverse effect. In addition, the effect of dynamic load on excitation frequency ratio can also be seen in Fig. 2. When the dynamic load parameter increases, the upper excitation frequency ratio increases and the lower excitation frequency ratio decreases. Table 7 lists the effect of compressive static load on excitation frequency ratio under various dynamic loads. It can be seen that the compressive static load reduces the excitation frequency ratio, and the larger the compressive static load, the smaller the excitation frequency ratio. The table also shows that the onset of primary instability, where α_D=0, is reduced with an increasing compressive static load. The results in Figs. 1-2 and Table 7 show that the influence of dynamic load parameter on the excitation frequency ratio is more significant than that of static load parameter. This is due to that the dynamic resonance frequency is mainly controlled by the dynamic load parameter rather than the static load parameter. Same behaviors can also be observed in the laminated plates with different fiber volume fractions and hygrothermal conditions. It is attributable to that the excitation frequency ratio is independent of material and hygrothermal conditions.

Table 7 Effect of static load parameters on excitation frequency ratio (*a/b*=1, *a/h*=10, S =0)

α_D		α_s					
		0	0.1	0.2	0.3	0.4	0.5
0	Ω/ω_{nf}^U	2	1.8974	1.7889	1.6733	1.5492	1.4142
	Ω/ω_{nf}^L	2	1.8974	1.7889	1.6733	1.5492	1.4142
0.2	Ω/ω_{nf}^U	2.0976	2.0000	1.8974	1.7889	1.6733	1.5492
	Ω/ω_{nf}^L	1.8974	1.7889	1.6733	1.5492	1.4142	1.2649
0.4	Ω/ω_{nf}^U	2.190	2.0976	2.0000	1.8974	1.7889	1.6733
	Ω/ω_{nf}^L	1.7889	1.6733	1.5492	1.4142	1.2649	1.0954
0.8	Ω/ω_{nf}^U	2.3664	2.2803	2.1909	2.0976	2.0000	1.8974
	Ω/ω_{nf}^L	1.5492	1.4142	1.2649	1.0954	0.8944	0.6325

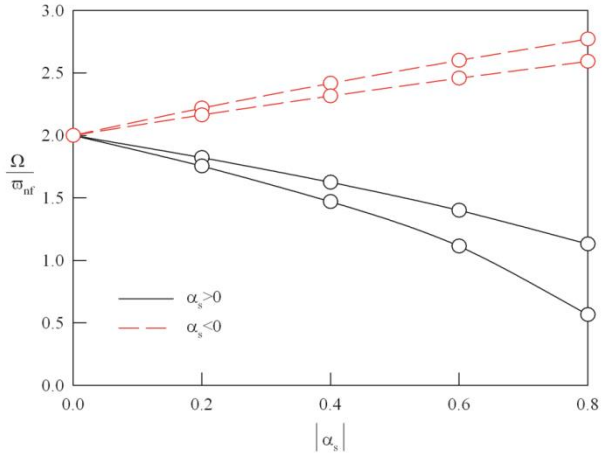

Fig. 1 Effect of static load types on excitation frequency ratio (*a/b*=1, *a/h*=10, $\alpha_D/|\alpha_s|$=0.3, *S*=0)

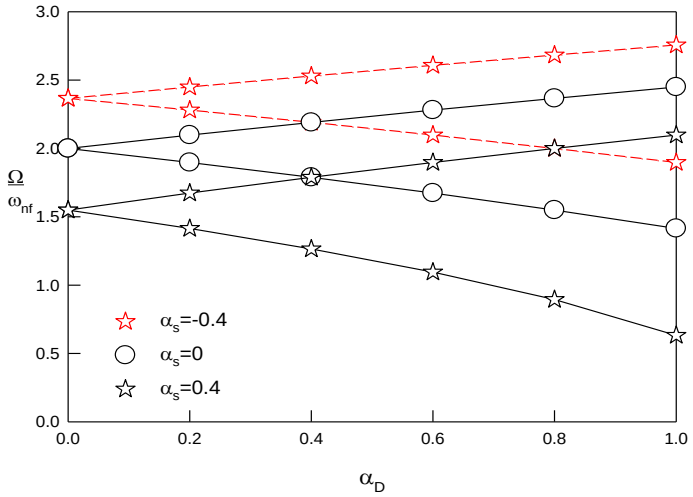

Fig. 2 Effect of dynamic load parameters on excitation frequency ratio (*a*/*b*=1, *a*/*h*=10, *S* =0)

Table 8 Hygrothermal effects on the dynamic stability of a laminated plate with various compressive static loads (*a*/*b*=1, *a*/*h*=10, V_f=0.5, *S*=0, α_D/α_s =0.3)

	ΔC	ΔT	α_s				
			0	0.2	0.4	0.6	0.8
$\Delta\Omega$	0	0	0	1.3502	3.1214	5.7643	11.3836
	1	0	0	1.2944	2.9926	5.5264	10.9138
	2	0	0	1.2399	2.8665	5.2936	10.4540
	3	0	0	1.1867	2.7435	5.0664	10.0053
	3	50	0	1.1793	2.7264	5.0347	9.9428
	3	100	0	1.1712	2.7077	5.0003	9.8747
	3	150	0	1.1624	2.6873	4.9626	9.8003
Ω_{DI}	0	0	0	0.1940	0.4485	0.8283	1.6357
	1	0	0	0.2111	0.4880	0.9011	1.7796
	2	0	0	0.2300	0.5318	0.9821	1.9396
	3	0	0	0.2511	0.5806	1.0722	2.1174
	3	50	0	0.2543	0.5879	1.0857	2.1442
	3	100	0	0.2578	0.5961	1.1008	2.1738
	3	150	0	0.2618	0.6052	1.1175	2.2069

In hygrothermal environmental conditions, the effects of static load parameter α_s on the instability region and the dynamic instability index of laminated plates (V_f=0.5) are shown in Tables 8-9. The static load parameter varies from 0 to 0.8 and the ratio of α_D/α_s is kept as 0.3. Increasing the static load will increase instability region and dynamic instability index. The temperature or/and moisture rise decrease instability region, but increase dynamic instability index. It can also be seen that the laminated plate under compressive static load (α_s >0) is more dynamically unstable than that under tensile load (α_s <0). In a uniform hygrothermal condition, the

Table 9 Hygrothermal effects on the dynamic stability of a laminated plate with various tensile static loads (a/b=1, a/h=10, V_f =0.5, S=0, α_D/α_s =0.3)

	ΔC	ΔT	α_s				
			0	-0.2	-0.4	-0.6	-0.8
$\Delta\Omega$	0	0	0	1.1023	2.0414	2.8648	3.6018
	1	0	0	1.0568	1.9571	2.7465	3.4532
	2	0	0	1.0123	1.8747	2.6308	3.3077
	3	0	0	0.9688	1.7942	2.5179	3.1657
	3	50	0	0.9628	1.7830	2.5022	3.1459
	3	100	0	0.9562	1.7708	2.4850	3.1244
	3	150	0	0.9490	1.7574	2.4663	3.1009
Ω_{DI}	0	0	0	0.1584	0.2933	0.4116	0.5176
	1	0	0	0.1723	0.3191	0.4478	0.5631
	2	0	0	0.1878	0.3478	0.4881	0.6137
	3	0	0	0.2050	0.3797	0.5329	0.6700
	3	50	0	0.2076	0.3845	0.5396	0.6784
	3	100	0	0.2105	0.3898	0.5471	0.6878
	3	150	0	0.2137	0.3958	0.5554	0.6983

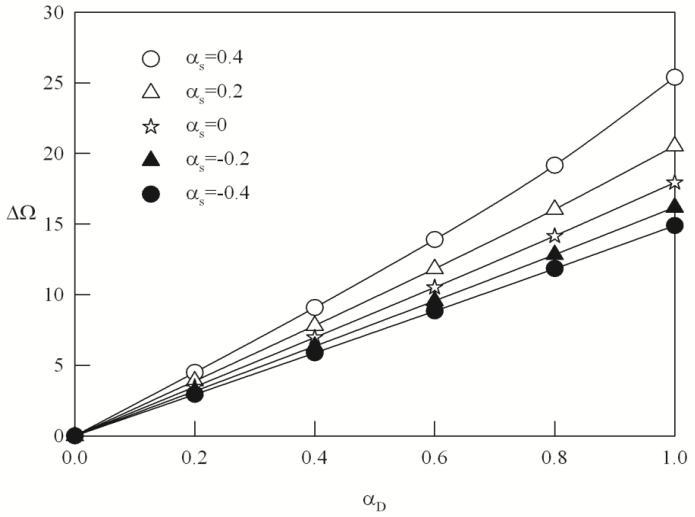

Fig. 3 Effect of dynamic load parameters on the instability region for various static load parameters (a/b=1, a/h=10, ΔT=150 $^{\circ}C$, ΔC=3%, V_f=0.5)

effects of static and dynamic load parameter on the instability region and dynamic instability index of laminated plates are shown in Figs. 3-4. As the dynamic load parameter increases, the width of the instability region zone and dynamic instability index increase. The instability region and dynamic instability index becomes much wider at higher dynamic load parameter. The influence of the dynamic load parameter on dynamic instability index is more apparent than the static load parameter.

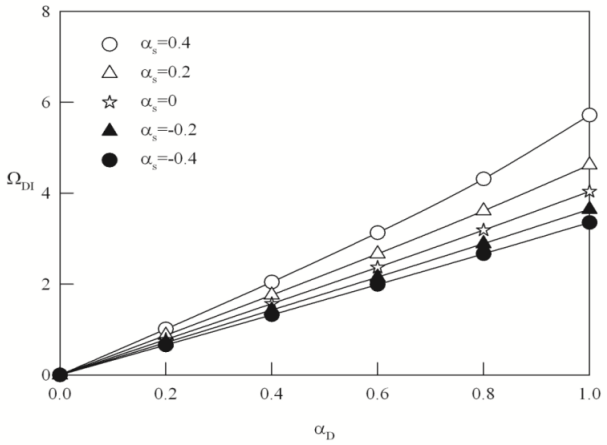

Fig. 4 Effect of dynamic load parameters on the dynamic instability index for various static load parameters (a/b=1, a/h=10, ΔT=150 $^{\circ}C$, ΔC=3%, V_f=0.5)

Table 10 Hygrothermal effects on the dynamic stability of a laminated plate with various dynamic loads (a/b=1, a/h=10, S=0, α_s=0.3)

	V_f	ΔC	ΔT	α_D				
				0	0.4	0.8	1.2	1.6
$\Delta\Omega$	0	0	0	0	3.4339	6.9803	10.8040	15.2791
	0.1	0	0	0	5.0922	10.3512	16.0215	22.6578
	0.3	0	0	0	6.8632	13.9511	21.5933	30.5376
	0.5	0	0	0	8.0904	16.4457	25.4545	35.9981
	0.5	1	0	0	7.7565	15.7670	24.4039	34.5124
	0.5	2	0	0	7.4297	15.1028	23.3759	33.0585
	0.5	3	0	0	7.1109	14.4546	22.3727	31.6397
	0.5	3	50	0	7.0664	14.3642	22.2327	31.4418
	0.5	3	100	0	7.0180	14.2658	22.0804	31.2264
	0.5	3	150	0	6.9651	14.1584	21.9142	30.9913
Ω_{DI}	0	0	0	0	7.9317	16.1231	24.9551	35.2917
	0.1	0	0	0	3.4488	7.0107	10.8510	15.3456
	0.3	0	0	0	1.7456	3.5484	5.4922	7.7671
	0.5	0	0	0	1.1625	2.3631	3.6576	5.1727
	0.5	1	0	0	1.2648	2.5710	3.9793	5.6276
	0.5	2	0	0	1.3785	2.8021	4.3370	6.1335
	0.5	3	0	0	1.5048	3.0590	4.7346	6.6958
	0.5	3	50	0	1.5239	3.0976	4.7945	6.7804
	0.5	3	100	0	1.5450	3.1405	4.8608	6.8743
	0.5	3	150	0	1.5685	3.1883	4.9348	6.9789

In hygrothermal conditions, the effects of static load on the instability region and dynamic instability index of laminated plates with various fiber volume fractions are shown in Figs. 5-6. It can be seen that as the fiber volume fraction increases, the instability region and the dynamic instability index decreases. It is due to that increasing fiber volume fraction will increase the

vibration frequency and critical buckling load, but decrease the value of dynamic instability index. For laminated plates with various fiber volume fractions, the compressive static load parameters produce a greater influence than the tensile load on the instability region and dynamic instability index. Thus, the dynamic instability of laminate plates is significantly affected by the fiber volume fraction, static and dynamic load parameters. The effect of fiber volume fraction and hygrothermal condition on instability region and dynamic instability index is shown in Table 10. The region of instability becomes much wider at higher dynamic load parameter, and without moisture and temperature (V_f =0.5, ΔT=0 $^\circ C$, ΔC= 0%), however, the dynamic instability index is smaller at the same conditions. A higher moisture or/and temperature rise leads to a smaller instability region and larger dynamic instability index, but higher fiber volume fraction has a reverse effect. Laminated plates become more dynamically unstable as moisture or/and temperature increases in the larger dynamic load parameters.

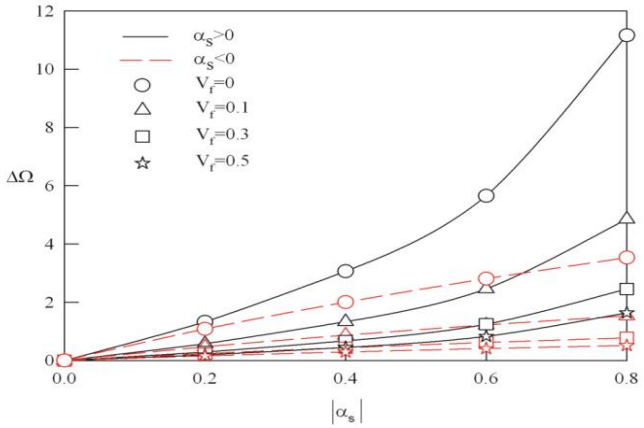

Fig. 5 Effect of static load on the instability region for different fiber volume fractions (*a/b*=1, *a/h*=10, ΔT=0, ΔC=0, S=0)

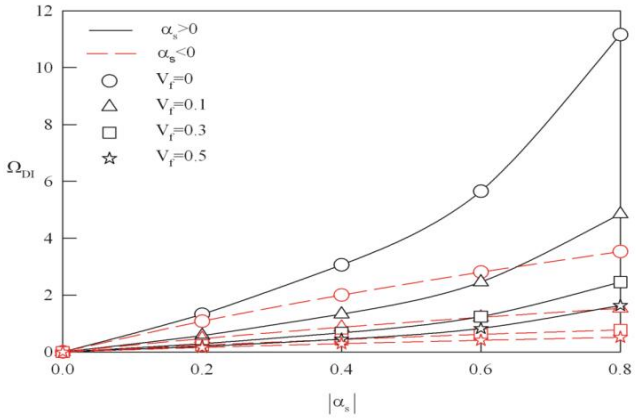

Fig. 6 Effect of α_s static load on the dynamic instability index for different fiber volume fractions(*a/b*=1, *a/h*=10, ΔT=0, ΔC=0, *S*=0)

Table 11 Effect of static load on the instability regions $\Delta\Omega$ of a laminated plate under various hygrothermal conditions. (a/b=1, a/h=10, V_f=0.5, S=0)

α_S	ΔC	ΔT	α_D				
			0	0.4	0.8	1.2	1.6
0.1	0	0	0	8.5384	17.4298	27.2482	39.7486
	1	0	0	8.1860	16.7104	26.1236	38.1081
	3	0	0	7.5046	15.3195	23.9492	34.9361
	3	50	0	7.4577	15.2237	23.7994	34.7176
	3	150	0	7.3508	15.0056	23.4584	34.2202
0	0	0	0	8.0904	16.4457	25.4545	35.9981
	1	0	0	7.7565	15.7670	24.4039	34.5124
	3	0	0	7.1109	14.4546	22.3727	31.6397
	3	50	0	7.0664	14.3642	22.2327	31.4418
	3	150	0	6.9651	14.1584	21.9142	30.9913
-0.1	0	0	0	7.7070	15.6193	24.0168	33.4325
	1	0	0	7.3889	14.9746	23.0256	32.0527
	3	0	0	6.7739	13.7282	21.1091	29.3848
	3	50	0	6.7315	13.6424	20.9770	29.2010
	3	150	0	6.6351	13.4469	20.6765	28.7826

Table 12 Effect of static load on the dynamic instability index of a laminated plate with various hygrothermal conditions. (a/b=1, a/h=10, V_f=0.5, S=0)

α_S	ΔC	ΔT	α_D				
			0	0.4	0.8	1.2	1.6
0.1	0	0	0	1.2269	2.5045	3.9154	5.7116
	1	0	0	1.3348	2.7248	4.2597	6.2139
	3	0	0	1.5882	3.2420	5.0683	7.3934
	3	50	0	1.6082	3.2830	5.1323	7.4868
	3	150	0	1.6553	3.3791	5.2826	7.7060
0	0	0	0	1.1625	2.3631	3.6576	5.1727
	1	0	0	1.2648	2.5710	3.9793	5.6276
	3	0	0	1.5048	3.0590	4.7346	6.6958
	3	50	0	1.5239	3.0976	4.7945	6.7804
	3	150	0	1.5685	3.1883	4.9348	6.9789
-0.1	0	0	0	1.1074	2.2444	3.4510	4.8040
	1	0	0	1.2048	2.4418	3.7545	5.2265
	3	0	0	1.4335	2.9053	4.4672	6.2186
	3	50	0	1.4517	2.9420	4.5237	6.2972
	3	150	0	1.4942	3.0281	4.6561	6.4816

The effects of static loading type and fiber volume fraction on the dynamic instability of laminated plates are presented in Tables 11-12. It shows that increasing fiber volume fraction will increase instability region and decrease dynamic instability index. The moisture or/and temperature has a soften effect on instability region and strengthen effect on dynamic instability index for any static loading type. The effects of dynamic load parameters and hygrothermal conditions on instability region and dynamic instability index are demonstrated in Figs. 7-8. The results are similar to those in Tables 11-12, the dynamic instability is mainly affected by the

dynamic load parameter in high moisture and temperature condition. The instability region and dynamic instability index increase when the moisture or/and temperature increases. The laminated plate becomes dynamically unstable at high moisture, temperature and dynamic load. The effects of bending stress ratio on the instability region and dynamic instability index of laminate plates are presented in Tables 13-16. The compressive static load has a strengthen effect on the instability region and dynamic instability index, but tensile static load has a reverse influence. The influence of dynamic load on dynamic instability is similar to compressive static load. A large bending stress slightly reduces the instability region and dynamic instability index.

Table 13 Effect of bending stress ratio on the instability regions of a laminate plate with various fiber volume fractions (a/b=1, a/h=10, ΔT=150 ^{o}C , ΔC=3%, α_D/α_S=0.3)

α_S	V_f	S				
		0	10	20	30	40
0.4	0	0.6018	0.6029	0.6062	0.6118	0.6196
	0.2	1.9541	1.9596	1.9760	2.0036	2.0425
	0.4	2.4807	2.4863	2.5031	2.5313	2.5710
-0.4	0	0.3935	0.3930	0.3913	0.3884	0.3844
	0.2	1.2780	1.2752	1.2667	1.2525	1.2325
	0.4	1.6224	1.6195	1.6108	1.5963	1.5759

Table 14 Effect of bending stress ratio on the dynamic instability index of a laminate plate with various fiber volume fractions (a/b=1, a/h=10, ΔT =150 ^{o}C , ΔC =3%, α_D/α_S =0.3)

α_S	V_f	S				
		0	10	20	30	40
0.4	0	14.8333	14.8605	14.9424	15.0793	15.2716
	0.2	1.2886	1.2922	1.3030	1.3212	1.3468
	0.4	0.7376	0.7393	0.7443	0.7526	0.7645
-0.4	0	9.7007	9.6866	9.6444	9.5738	9.4749
	0.2	0.8427	0.8408	0.8352	0.8259	0.8127
	0.4	0.4824	0.4815	0.4790	0.4746	0.4686

Table 15 Effect of the bending stress ratio on the dynamic instability under various dynamic loads S (a/b=1, a/h=10, ΔT=150 ^{o}C , ΔC=3%, α_s=-0.4)

α_D	V_f	S				
		0	10	20	30	40
0.2	0	0.6562	0.6552	0.6524	0.6476	0.6409
	0.2	2.1308	2.1261	2.1120	2.0884	2.0552
	0.4	2.7051	2.7003	2.6858	2.6617	2.6277
0.4	0	1.3149	1.3130	1.3074	1.2979	1.2847
	0.2	4.2699	4.2606	4.2326	4.1858	4.1199
	0.4	5.4206	5.4111	5.3825	5.3346	5.2672
0.6	0	1.9788	1.9760	1.9677	1.9537	1.9342
	0.2	6.4258	6.4121	6.3708	6.3015	6.2040
	0.4	8.1575	8.1434	8.1012	8.0304	7.9306

Table 16 Effect of the bending stress ratio on the dynamic instability index under various dynamic loads S (a/b=1, a/h=10, ΔT=150 $^{\circ}C$, ΔC=3%, α_s=-0.4)

α_D	V_f	S				
		0	10	20	30	40
0.2	0	16.1745	16.1511	16.0807	15.9634	15.7989
	0.2	1.4051	1.4020	1.3927	1.3771	1.3552
	0.4	0.8043	0.8029	0.7986	0.7914	0.7813
0.4	0	32.4115	32.3651	32.2257	31.9931	31.6670
	0.2	2.8156	2.8094	2.7910	2.7601	2.7167
	0.4	1.6117	1.6089	1.6004	1.5862	1.5661
0.6	0	48.7765	48.7080	48.5022	48.1587	47.6769
	0.2	4.2372	4.2282	4.2009	4.1553	4.0909
	0.4	2.4255	2.4214	2.4088	2.3878	2.3581

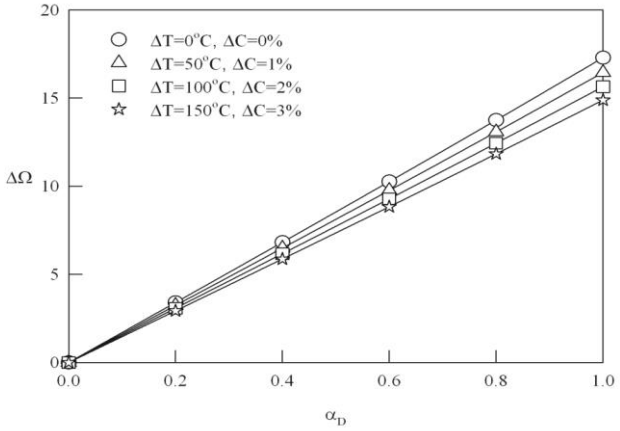

Fig. 7 Hygrothermal effects on the instability region for various dynamic load parameters (a/b=1, a/h=10, V_f=0.5, α_s=-0.4, S=0)

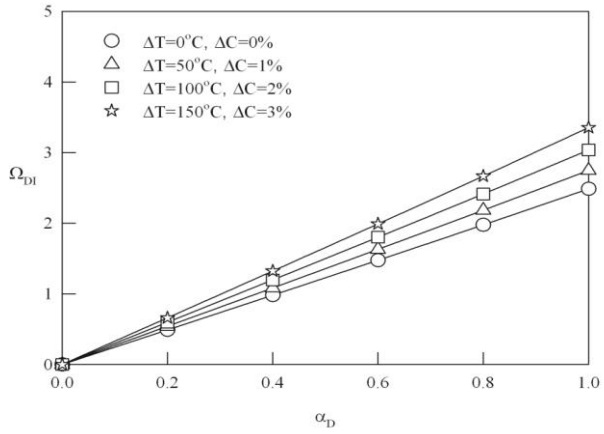

Fig. 8 Hygrothermal effects on the dynamic instability index for various dynamic load parameters (a/b=1, a/h=10, V_f =0.5, α_s=-0.4, S=0)

5. Conclusions

The hygrothermal dynamic stability of laminate plates subjected to periodic loads is described and discussed in this paper. The dynamic instability is sensitive to the hygrothermal load and periodic dynamic loads. Based on above discussions, the preliminary results are summarized as follows:

• The buckling load and vibration frequency of laminated plates are affected by the moisture, temperature and fiber volume fraction. The buckling load and vibration frequency decrease as moisture and temperature increase, or fiber volume fraction decreases.

• The excitation frequency ratio and the onset of instability are affected by static loads, but they are independent of material and hygrothermal conditions. Compressive loads reduce the excitation frequency ratio and the onset of instability, but tensile loads increase them.

• The instability region and dynamic instability index are significantly affected by temperature, moisture, fiber volume fraction, static load and dynamic load, but they are slightly affected by bending stress. The temperature or/and moisture rise decrease instability region and increase dynamic instability index, but higher fiber volume fraction has a reverse effect. The compressive static load has a strengthen effect on the instability region and dynamic instability index, but tensile static load has a reverse influence. The laminated plate with various fiber volume fractions under compressive static load is more dynamically unstable than that under tensile static load. The instability region and dynamic instability index increase with the dynamic load, and the influence of the dynamic load on dynamic instability index is more apparent than the static load.

References

Adams, D.F. and Miller, A.K. (1977), "Hygrothermal microstresses in a unidirectional composite exhibiting inelastic materials behavior", *J. Compos. Mater.*, **11**, 285-299.

Bolotin, V.V. (1964), *The dynamic stability of elastic systems*, Holden-Day, San Francisco, CA.

Bowles, D.E. and Tompkins, S.S. (1989), "Prediction of coefficients of thermal expansion for unidirectional composites", *J. Compos. Mater.*, **23**, 370-381.

Brunell, E.J. and Robertson, S.R. (1974), "Initially stressed Mindlin plates", *AIAA J.*, **12**, 1036-1045.

Chakrabarti, A. (2008), "An efficient FE model for dynamic instability analysis of imperfect composite laminates", *Struct. Eng. Mech.*, **30**, 383-386.

Chen, C.S., Fung, C.P. and Chien, R.D. (2006), "A further study on nonlinear vibration of initially stressed plates", *Appl. Math. and Comput.*, **172**, 349-367.

Chen, C.S., Chen, W.R. and Chien, R.D. (2009), "Stability of parametric vibrations of hybrid laminated plates", *Eur. J. Mech. A- Solids*, **28**, 329-337.

Chen, C.S., Tsai, T.C.**,** Chen, W.R. and Wei, C.L. (2013), "Dynamic analysis of laminated composite plates in thermal environments", *Steel Compos. Struct.*, **15**, 57-79.

Chen, L.W. and Yang, J.Y. (1990), "Dynamic stability of laminated composite plates by the finite element method", *Comput. Struct.*, **36**, 845-851.

Cho, H.K. (2009), "Optimization of dynamic behaviors of an orthotropic composite shell subjected to hygrothermal environment", *Finite Elem. Anal. Des.*, **45**, 852-860.

Dey, P. and Sinqha, M.K. (2006), "Dynamic stability analysis of composite skew plates subjected to periodic in-plane load", *Thin Wall. Struct.*, **44**, 937-942.

Evan-Ivanowski, R.M. (1976), *Resonance oscillations in mechanical systems*, Elsevier, Amsterdam.

Gigliottia, M., Molimard, J., Jacquemin, F. and Vautrin, A. (2006), "On the nonlinear deformations of thin unsymmetric 0/90 composite plates under hygrothermal loads", *Compos. Part A- Appl. Sci. Manuf.*, **37**,

624-629.
Huang, X.L., Shen, H.S. and Zheng, J.J. (2004), "Nonlinear vibration and dynamic response of shear deformable laminated plates in hygrothermal environments", *Compos. Sci. Tech.*, **64**, 1419-1435.
Kumar, R. and Singh, D. (2012), "Hygrothermal buckling response of laminated composite plates with random material properties: Micro-mechanical model", *Appl. Mech. Mater.*, **110-116**, 113-119.
Liu, C.F. and Huang, C.H. (1996), "Free vibration of composite laminated plates subjected to temperature changes", *Comput. Struct.*, **60**, 95-101.
Nanda, N. and Pradyumna, S. (2011), "Nonlinear dynamic response of laminated shells with imperfections in hygrothermal environments", *J. Compos. Mater.*, **45**, 2103-2112.
Parhi, P.K., Bhattacharyya, S.K. and Sinha, P.K. (2001), "Hygrothermal effects on the dynamic behavior of multiple delaminated composite plates and shells", *J. Sound Vib.*, **248**, 195-214.
Patel, B.P., Ganapathi, M. and Makhecha, D.P. (2002), "Hygrothermal effects on the structural behaviour of thick composite laminates using higher-order theory", *Compos. Struct.*, **56**, 25-34.
Patel, S.N., Datta, P.K. and Sheikh, A.H. (2009), "Parametric study on the dynamic instability behavior of laminated composite stiffened plate", *J. Eng. Mech.*, **135**, 1331-1341.
Raja, S., Sinha, P.K., Prathap, G. and Dwaeakanathan, D. (2004), "Influence of active stiffening on dynamic behaviour of piezo-hygro-thermo-elastic composite plates and shells", *J. Sound Vib.*, **278**, 257-283.
Rao, V.V.S. and Sinha, P.K. (2004a), "Bending characteristics of thick multidirectional composite plates under hygrothermal environment", *J. Reinf. Plast. Compos.*, **23**, 1481-1495.
Rao, V.V.S. and Sinha, P.K. (2004b), "Dynamic response of multidirectional composites in hygrothermal environments", *Compos. Struct.*, **64**, 329-338.
Shen, H.S. (2001), "Hygrothermal effects on the postbuckling of shear deformable laminated plates", *Int. J. Mech. Sci.*, **43**, 1259-1281.
Shen, H.S., Zheng, J.J. and Huang, X.L. (2004), "The effects of hygrothermal conditions on the dynamic response of shear deformable laminated plates resting on elastic foundations", *J. Reinf. Plast. Compos.*, **23**, 1095-1113.
Tsai, S.W. and Hahn, H.T. (1980), *Introduction to composite materials*, Technomic Publishing Co, Westport, CT.
Wang, S. and Dawe, D.J. (2002), "Dynamic instability of composite laminated rectangular plates and prismatic plate structures", *Comput. Meth. Appl. Mech. Eng.*, **191**, 1791-1826.

Appendix

$$L_1 = A_{11}\, u_{x,x} + A_{16}\,(u_{x,y} + u_{y,x}) + A_{12}\, u_{y,y} + B_{11}\, \varphi_{x,x} + B_{16}\,(\varphi_{x,y} + \varphi_{y,x}) + B_{12}\, \varphi_{y,y}$$

$$L_2 = A_{16}\, u_{x,x} + A_{26}\, u_{y,y} + A_{66}\,(u_{x,y} + u_{y,x}) + B_{16}\, \varphi_{x,x} + B_{66}\,(\varphi_{x,y} + \varphi_{y,x}) + B_{26}\, \varphi_{y,y}$$

$$L_3 = A_{12}\, u_{x,x} + A_{26}\,(u_{x,y} + u_{y,x}) + A_{22}\, u_{y,y} + B_{12}\, \varphi_{x,x} + B_{26}\,(\varphi_{x,y} + \varphi_{y,x}) + B_{22}\, \varphi_{y,y}$$

$$L_4 = A_{55}\,(w_{,x} + \varphi_x) + A_{45}\,(w_{,y} + \varphi_y)$$

$$L_5 = A_{45}\,(w_{,x} + \varphi_x) + A_{44}\,(w_{,y} + \varphi_y)$$

$$L_6 = B_{11}\mathrm{u}_{x,x} + B_{16}\,(u_{x,y} + u_{y,x}) + B_{12}\, \varphi_{y,y} + D_{11}\varphi_{x,x} + D_{16}\,(\varphi_{x,y} + \varphi_{y,x}) + D_{12}\, \varphi_{y,y}$$

$$L_7 = B_{16}\, u_{x,x} + B_{66}\,(\mathrm{u}_{x,y} + \mathrm{u}_{y,x}) + B_{26}\, u_{y,y} + D_{16}\, \varphi_{x,x} + D_{66}\,(\varphi_{x,y} + \varphi_{y,x}) + D_{22}\, \varphi_{y,y}$$

$$L_8 = A_{45}\,(w_{,y} + \varphi_y) + A_{55}\,(w_{,x} + \varphi_x)$$

$$L_9 = B_{12}\mathrm{u}_{x,x} + B_{22}\,\mathrm{u}_{y,y} + B_{26}\,(u_{x,y} + u_{y,x}) + D_{12}\, \varphi_{x,x} + D_{26}\,(\varphi_{x,y} + \varphi_{y,x}) + D_{22}\, \varphi_{y,y}$$

$$L_{10} = A_{44}\,(w_{,y} + \varphi_y) + A_{45}\,(w_{,x} + \varphi_x)$$

$$P_1 = N_{xx}u_{x,x} + M_{xx}\varphi_{x,x} + N_{xy}u_{x,y} + M_{xy}\varphi_{x,y} + N_{xz}u_{z,x}$$

$$P_2 = N_{yy}u_{x,y} + M_{yy}\varphi_{x,y} + N_{xy}u_{x,x} + M_{xy}\varphi_{x,x} + N_{yz}u_{z,x}$$

$$P_3 = N_{xx}u_{y,x} + M_{xx}\varphi_{y,x} + N_{xy}u_{y,y} + M_{xy}\varphi_{y,y} + N_{xz}u_{z,y}$$

$$P_4 = N_{yy}u_{y,y} + M_{yy}\varphi_{y,y} + N_{xy}u_{y,x} + M_{xy}\varphi_{y,x} + N_{xz}u_{z,y}$$

$$P_5 = N_{xx}w_{,x} + N_{xy}w_{,y}$$

$$P_6 = N_{xy}w_{,x} + N_{yy}w_{,y}$$

$$P_7 = M_{xx}u_{x,x} + M^{*}_{xx}\varphi_{x,x} + M_{xy}u_{x,y} + M^{*}_{xy}\varphi_{x,y} + M_{xz}u_{z,x}$$

$$P_8 = M_{yy}u_{x,y} + M^{*}_{yy}\varphi_{x,y} + M_{xy}u_{x,x} + M^{*}_{xy}\varphi_{x,x} + M_{yz}u_{z,x}$$

$$P_9 = N_{xz}u_{x,x} + M_{xz}\varphi_{x,x} + N_{zz}\varphi_x + N_{zy}u_{x,y} + M_{zy}\varphi_{x,y}$$

$$P_{10} = M_{xx}u_{y,x} + M^{*}_{xx}\varphi_{y,x} + M_{xy}u_{y,y} + M^{*}_{xy}\varphi_{y,y} + M_{xz}u_{z,y}$$

$$P_{11} = M_{yy}u_{y,y} + M^{*}_{yy}\varphi_{y,y} + M_{xy}\varphi_{y,x} + M^{*}_{xy}u_{y,x} + M_{xz}u_{z,y}$$

$$P_{12} = N_{xz}u_{y,x} + M_{xz}\varphi_{y,x} + N_{zz}\varphi_y + N_{zy}u_{y,y} + M_{zy}\varphi_{y,y}$$

$$T_1 = N^{T}_{XX}u_{x,x} + M^{T}_{xx}\varphi_{x,x} + N^{T}_{xy}u_{x,y} + M^{T}_{xy}\varphi_{x,y}$$

$$T_2 = N^{T}_{yy}u_{x,y} + M^{T}_{yy}\varphi_{x,y} + N^{T}_{xy}u_{x,x} + M^{T}_{xy}\varphi_{x,x}$$

$$T_3 = N^{T}_{xx}u_{y,x} + M^{T}_{xx}\varphi_{y,x} + N^{T}_{xy}u_{y,y} + M^{T}_{xy}\varphi_{y,y}$$

$$T_4 = N^{T}_{yy}u_{y,y} + M^{T}_{yy}\varphi_{y,y} + N^{T}_{xy}u_{y,x} + M^{T}_{xy}\varphi_{y,x}$$

$$T_5 = N^{T}_{xx}w_{,x} + N^{T}_{xy}w_{,y}$$

$$H_5 = N^{H}_{xx}w_{,x} + N^{H}_{xy}w_{,y}$$

$$T_6 = N^{T}_{xy}w_{,x} + N^{T}_{yy}w_{,y}$$

$$T_7 = M^T_{xx} u_{x,x} + M^{T*}_{xx} \varphi_{x,x} + M^T_{xy} u_{x,y} + M^{T*}_{xy} \varphi_{x,y}$$

$$T_8 = M^T_{yy} u_{x,y} + M^{T*}_{yy} \varphi_{x,y} + M^T_{xy} u_{x,x} + M^{T*}_{xy} \varphi_{x,x}$$

$$T_9 = M^T_{xx} u_{y,x} + M^{T*}_{xx} \varphi_{y,x} + M^T_{xy} u_{y,y} + M^{T*}_{xy} \varphi_{y,y}$$

$$T_{10} = M^T_{yy} u_{y,y} + M^{T*}_{yy} \varphi_{y,y} + M^T_{xy} \varphi_{y,x} + M^{T*}_{xy} u_{y,x}$$

$$H_1 = N^{\mathrm{H}}_{XX} u_{x,x} + M^H_{xx} \varphi_{x,x} + N^H_{xy} u_{x,y} + M^H_{xy} \varphi_{x,y}$$

$$H_2 = N^H_{yy} u_{x,y} + M^H_{yy} \varphi_{x,y} + N^H_{xy} u_{x,x} + M^H_{xy} \varphi_{x,x}$$

$$H_3 = N^H_{xx} u_{y,x} + M^H_{xx} \varphi_{y,x} + N^H_{xy} u_{y,y} + M^H_{xy} \varphi_{y,y}$$

$$H_4 = N^H_{yy} u_{y,y} + M^H_{yy} \varphi_{y,y} + N^H_{xy} u_{y,x} + M^H_{xy} \varphi_{y,x}$$

$$H_6 = N^H_{xy} w_{,x} + N^H_{yy} w_{,y}$$

$$H_7 = M^H_{xx} u_{x,x} + M^{H*}_{xx} \varphi_{x,x} + M^H_{xy} u_{x,y} + M^{H*}_{xy} \varphi_{x,y}$$

$$H_8 = M^H_{yy} u_{x,y} + M^{H*}_{yy} \varphi_{x,y} + M^H_{xy} u_{x,x} + M^{H*}_{xy} \varphi_{x,x}$$

$$H_9 = M^H_{xx} u_{y,x} + M^{H*}_{xx} \varphi_{y,x} + M^H_{xy} u_{y,y} + M^{H*}_{xy} \varphi_{y,y}$$

$$H_{10} = M^H_{yy} u_{y,y} + M^{H*}_{yy} \varphi_{y,y} + M^H_{xy} \varphi_{y,x} + M^{H*}_{xy} u_{y,x}$$

where

$$(\mathrm{A_{ij}}, \mathrm{B_{ij}}, \mathrm{D_{ij}}) = \int C_{ij} (1, z, z^2)\, dz \quad (i, j = 1, 2, 4, 5, 6)$$

$$(N_{ij}, M_{ij}, M^*_{ij}) = \int \sigma_{\mathrm{ij}} (1, z, z^2)\, dz \quad (i, j = x, y, z)$$

$$(N^T_{ij}, M^T_{ij}, M^{T*}_{ij}) = -\int \alpha_{ij} C_{ij} \Delta T (1, z, z^2)\, dz \quad (i = x, y)$$

$$(N^H_{ij}, M^H_{ij}, M^{H*}_{ij}) = -\int \beta_{ij} C_{ij} \Delta C (1, z, z^2)\, dz \quad (i = x, y)$$

$$(I_1, I_3) = \int \rho(z) (1, z^2)\, dz$$

$$f_i = \int_{-h/2}^{h/2} (\bar{X}_i + \Delta X_i)\, dz + \sigma^+_{zi} - \sigma^-_{zi} \quad (i = x, y)$$

$$f_z = \int_{-h/2}^{h/2} (\bar{X}_z + \Delta X_z)\, dz + (\sigma^+_{zx} - \sigma^-_{zx}) w_{,x} + (\sigma^+_{zy} - \sigma^-_{zy}) w_{,y} + \sigma^+_{zz} - \sigma^-_{zz}$$

$$m_i = \int_{-h/2}^{h/2} (\bar{X}_i + \Delta X_i)\, z dz + h (\sigma^+_{zi} - \sigma^-_{zi})/2 \qquad (i = x, y)$$

Here C_{ij}'s are the elastic constant of the stiffness matrix; ρ is the mass density; A_{ij}, B_{ij} and D_{ij} are the laminate stiffness coefficients; N_{ij}, M_{ij} and M^*_{ij} are arbitrary initial stress resultants. The N^T_{ij}, M^T_{ij} and M^{T*}_{jj} are thermal stresses, The N^H_{ij}, M^H_{ij} and M^{H*}_{jj} are humid stresses resultants. f_x, f_y, f_z, m_x and m_y are the loads comprising lateral loads at the top and bottom face of the plate and the body

force. The superscripts '+' and '-' denote the stresses evaluated at the top and bottom face of the plate, respectively. Meanwhile, all the integrations are performed through the thickness of the plate from -*h*/2 to *h*/2.